Biomass and Bioenergy 193 (2025) 107572

Contents lists available at ScienceDirect

Biomass and Bioenergy

journal homepage: www.elsevier.com/locate/biombioe

Use of methanol as a promoter for ammonia combustion

A. Ruiz-Gutiérrez, I. De Diego, M.U. Alzueta *

Aragón Institute of Engineering Research (I3A), Department of Chemical and Environmental Engineering, University of Zaragoza, 50018, Zaragoza, Spain

ARTICLE INFO

Keywords:
NH_3
Ammonia
CH_3OH
Methanol
NH_3/CH_3OH mixtures
Kinetic modelling

ABSTRACT

This work aims to study the oxidation of ammonia and methanol mixtures (NH_3/CH_3OH). For this purpose, laboratory experiments were conducted using a quartz flow reactor at atmospheric pressure, in a temperature range of 875–1425 K. The oxygen excess ratio (λ) and the NH_3/CH_3OH ratio were modified during the experiments. The experimental results have been simulated with a literature-based kinetic mechanism. The results show that the presence of CH_3OH and the oxygen excess ratio affect the conversion of NH_3, shifting its oxidation to lower temperatures as these variables increase. The oxidation of both fuels was slightly boosted with increasing CH_3OH concentration. The λ study showed that the fuel-lean conditions accelerate NH_3 oxidation at lower temperatures whereas do not have the same effect on CH_3OH oxidation. The H radical concentration significantly influences fuel consumption, especially in reactions involving CH_3OH and NH_2, and it is also key for inhibition processes. CH_3OH was found to initiate NH_3 reactions, with strong competition for OH radicals between the two fuels. Nevertheless, methanol helps reduce ammonia's oxidation temperature. CH_2OH was identified as the predominant species following H-abstraction from CH_3OH. In the NH_3/CH_3OH ratio studies, increasing methanol concentration lowered the oxidation temperature of both fuels, with a temperature difference of up to 150 K observed for NH_3/CH_3OH ratios from 0.6 to 10. Increasing methanol concentration for a given NH_3 value also shifted the prominence of secondary reaction pathways, further influencing the overall oxidation process.

1. Introduction

Combustion of NH_3 is gaining attention in the renewable energy sector [1], because NH_3 can be obtained from renewable sources and because ideal NH_3 combustion produces water and nitrogen, as non-harmful compounds to the environment. Moreover, NH_3 is an important hydrogen carrier. In addition, ammonia is a compound with a well-developed infrastructure, as since the discovery of the Haber-Bosch process, it has become one of the most widely produced compounds globally. This, in turn, means a high level of development in its storage methodology [2], since it can easily be stored in a liquid state, due to its unrestrictive condensation conditions. Although ammonia under atmospheric conditions is a colourless gas, its characteristic odour makes it easy to detect leakage, making it a compound safer than hydrogen.

Furthermore, NH_3 is not only produced by conventional techniques, as there are ways to yield it from renewable energy sources such as wind or solar energy [3], following the power-to-fuel strategy. NH_3 produced from such energy resources is called "green ammonia". However, as a non-carbon combustible, it has certain difficulties such as a low calorific value, low linear burning rate, poor flammability, and a high auto-ignition temperature [4].

One of the most extensive techniques to facilitate the ignition of ammonia is based on its mixing with other fuels with better ignition properties. The mixtures with oxygenated compounds have been considered in the past since a small proportion of oxygenated compounds mixed with carbon fuels leads, among other effects, to a decrease in soot formation, increases the anti-knock power of the gasoline and optimises combustion [5,6]. Some of the most studied oxygenated compounds are methanol (CH_3OH), dimethyl ether (DME) [7–15], dimethoxymethane (DMM) [16], diethyl ether (DEE) [17,18] or ethanol (C_2H_5OH) [19,20]. The NH_3-DME mixture is the most widely studied, while compounds such as CH_3OH or DEE have been scarcely considered to be mixed.

CH_3OH is an interesting candidate to be mixed with ammonia for different reasons: the high content of oxygen in the molecule, its simplicity compared to other oxygenates, its increasing availability for use, together with the various synthesis possibilities. In this context, biomethanol obtained from different sources may be an excellent candidate

* Corresponding author.
E-mail address: uxue@unizar.es (M.U. Alzueta).

https://doi.org/10.1016/j.biombioe.2024.107572
Received 15 November 2024; Received in revised form 19 December 2024; Accepted 19 December 2024
Available online 27 December 2024

for its blending with ammonia, in the progress for a sustainable and decarbonized economy. For example, bio-methanol can be produced through gasification of biomass residues or municipal waste, a must nowadays when producing biofuels. CH_3OH production from glycerine has also been reported (BioMCM, Netherlands), a subproduct of biodiesel synthesis [21]. The different CH_3OH synthesis methodologies are interesting but may be insufficient for full fuel supply, and techniques related to renewable energies and CO_2 capture have also been considered [21].

The presence of CH_3OH acts as an ignition booster since CH_3OH contributes to an increase in OH, O, H, and HO_2 radicals [22,23]. CH_3OH has been mentioned to contribute importantly to the formation of HO_2 radicals, which in turn promotes a higher production of OH radicals [24]. Part of the OH formed from methanol originates from the reaction $CH_3OH + HO_2 \rightleftharpoons CH_2OH + H_2O_2$ (r1). Subsequently, the hydrogen peroxide (H_2O_2) produced decomposes via H_2O_2 (+M) $\rightleftharpoons$ 2OH (+M) (r2), leading to a global increase in OH radicals in the mixture. This provides evidence of the effectiveness of CH_3OH as a promoter of fuel combustion in general and ammonia in particular, because the most relevant reaction in the ammonia conversion initiation, i.e. $NH_3 + OH \rightleftharpoons NH_2 + H_2O$ (r3), requires OH radicals. At the same time, the reaction $H + O_2 \rightleftharpoons OH + H$ (r4) remains fundamental to the combustion of both NH_3 and CH_3OH [23], since it feeds into the H/O radical pool and contributes to increasing the concentration of OH radicals through the following reactions: (r4) and $O + H_2O \rightleftharpoons 2OH$ (r5). These effects are amplified as conditions become fuel-leaner [25–27].

Studies have been conducted to evaluate various important combustion parameters, such as IDTs, pressure, temperature, and LBVs, for this fuel mixture. Regarding the IDTs studies, results have shown an improvement in this parameter with adding methanol. This establishes an inversely proportional relationship between the methanol concentration in the mixture and the IDT's values [1,28]. A pronounced increase in the concentration of CH_3OH (60–80%) does not significantly affect the reduction in the oxidation temperature of fuels (NH_3/CH_3OH) in function to pressure. In contrast, at lower methanol concentrations, pressure exerts a more substantial influence of pressure on the oxidation temperature of ammonia [1].

In LBVs studies, the behaviour of the mixture is corroborated, and improvements are observed with the addition of methanol [19,23]. This leads to a faster NH_3 consumption. For this parameter (LBVs), it is indicated that the most influential reaction is $H + O_2 \rightleftharpoons OH + O$ (r4), with no relevant C-N interactions observed [19].

Pressure studies have also been conducted for the NH_3/CH_3OH mixture [24,25,28], determining that methanol can reduce the temperature at which ammonia is oxidised, with NH_3 oxidation being shifted by over 100 K at 40 bar pressure and 1% CH_3OH [28]. However, the CH_3OH conversion is less influenced by pressure, showing only a 50 K difference in CH_3OH oxidation at a pressure difference of 80 bar [25]. This suggests that a higher proportion of CH_3OH in the fuel mixture may reduce the effect of pressure on the promoted oxidation of both NH_3 and CH_3OH. A compilation of published studies on the mixture can be found in Table S1 of the supplementary material.

In this context, the present study aims to achieve a better understanding of the conversion of the NH_3/CH_3OH mixture and the formation of products. To our knowledge, only a single study has been conducted in a flow reactor [24]. Yin et al. [24] focused on the effect of the NH_3/CH_3OH ratio, in a high pressure study, not addressing variation of λ were not considered. Therefore, the present work extends the range of operating conditions, to account for the effect of oxygen excess ratio, additionally to temperature and NH_3/CH_3OH ratio. Moreover, to our knowledge, this is the first work addressing the pyrolysis of NH_3/CH_3OH mixtures, which may be of interest for the near burner zones of practical devices. Additionally, not many studies have focused so far on the profiles of many of the species obtained during NH_3/CH_3OH oxidation [1,22,25]. Finally, this study can contribute to the development and a better understanding of kinetic models, with an emphasis on the reactions considered as the most important ones.

2. Experimental

The experiments have been carried out using a quartz flow reactor. The length and diameter of the reactor are 20 cm and 0.87 cm, respectively. This reactor is located inside an electric furnace with three heating zones. Isothermal conditions have been achieved within ±5 K. Temperature was measured every 2 cm using a type-K fine-wire thermocouple. The temperature profiles for the individual temperatures can be found in Fig. S1 of the Supplementary Material. Flow meters (Alicat) control the volumetric gas flow rates. Controllers are operated within the 10% and 90% of the nominal maximum flow rate of the controller to ensure an accurate measurement. To verify that these flow rates are accurate, a digital bubble meter (Agilent flow meter) is used at the same time. A total gas flow rate of 1000 mL min^{-1} (STP) was kept constant throughout the experiment. The gases added are Ar (99.9% purity), CH_3OH (0.002, 0.003%vol), NH_3 (1%vol) and O_2 (1.5–8.0%vol). All the compounds are diluted in argon and supplied by Nippon gases. The main gas in the mixtures will always be Ar, which will be preheated before mixing with other gases. The residence time is calculated with the volume reactor and gas flow rate, expressed as a function of operating temperature. A more detailed explanation of the experimental setup can be found in Alzueta et al. [29] and the schematic of the setup can be found in Fig. S2 of Supplementary Material.

The experimental parameters modified in the different experiments are temperature (825–1425 K), O_2 excess ratio (λ) and concentration ratio. All experimental sets are shown in Table 1 λ is the ratio between the feed O_2 and the stoichiometry O_2, and it is calculated according to the following chemical equations:

$$NH_3 + 0.75\ O_2 \rightarrow 0.5\ N_2 + 1.5H_2O \quad (1)$$

$$CH_3OH + 1.5\ O_2 \rightarrow CO_2 + 2H_2O \quad (2)$$

To measure the different compounds formed during the experiment, an Agilent 990C micro gas chromatograph is used. With this device it is possible to quantify H_2, O_2, N_2, CH_4, CO_2, C_2H_2, C_2H_4, C_2H_6, N_2O, NH_3, and HCN. The error has been calculated based on the standard deviation, and it does not vary with temperature within the considered interval. This represents an estimation of the experimental Micro GC error. The maximum uncertainty in the measurements for each temperature is ±10 ppm. In addition, the outlet gas stream is also analysed by an Advance Optima AO2020 continuous gas analyser, which measures the concentration of NO and NO_2. The NO analyser has an uncertainty of 1 %, but not less than 10 ppm. NO_2 concentrations were negligible in all the conditions studied.

In Table 2, sets 1 and 2 are pyrolysis experiments with different NH_3/CH_3OH mixture ratios to measure methanol influence on ammonia

Table 1
Experimental conditions. Balance is made with Ar and the flow rate is 1000 mL min^{-1} (STP). Concentrations are expressed in ppm.

Set	NH_3	CH_3OH	O_2	λ	NH_3/CH_3OH	t_r(s)
1	496	511	0	0.00	0.97	190.6/T(K)
2	229	507	0	0.00	0.50	190.1/T(K)
3	482	512	546	0.48	0.94	189.6/T(K)
4	461	493	1133	0.99	0.94	191.6/T(K)
4R	481	511	1126	1.00	0.94	188.8/T(K)
5	486	529	2138	2.00	0.92	189.6/T(K)
6	178	296	298	0.51	0.60	190.3/T(K)
7	189	304	560	0.94	0.62	191.4/T(K)
8	192	326	1222	1.92	0.60	190.3/T(K)
9	1010	107	452	0.49	9.43	190.6/T(K)
10	1009	106	905	1.01	9.53	189.6/T(K)
11	952	97	1766	1.99	9.84	190.3/T(K)
12	0	503	0	0	0	191.6/T(K)
13 [30]	1149	0	0	0	0	195.0/T(K)

Table 2
Added or modified equations in the mechanism. Rate constants are expressed as $A*T^n *exp(-E_a/RT)$. Units are calories, cm^3, mol, and second.

Reaction Mechanism	A	n	E_a	Ref.
$NH_2 + CH_3OH \rightleftharpoons NH_3 + CH_3O$ (r6)	1.86E00	3.59	2930	[25]
$NH_2 + CH_3OH \rightleftharpoons NH_3 + CH_2OH$ (r7)	7.44E00	3.64	4300	[25]
$NH_2 + CH_3OH \rightleftharpoons NH_2OH + CH_3$ (r8)	1.90E34	−6.34	67678	[28]
$NH_2 + CH_2OH \rightleftharpoons NH_3 + CH_2O$ (r9)	1.30E06	1.94	1150	[28]
$NH_2 + CH_2OH \rightleftharpoons NH + CH_3OH$ (r10)	5.60E06	1.94	14573	[28]
$NH_2 + CH_2OH \rightleftharpoons NH_3 + HCOH$ (r11)	3.20E06	1.87	7570	[28]
$NH_2 + CH_3O \rightleftharpoons NH_3 + CH_2O$ (r12)	3.30E06	1.94	−1150	[28]
$NH_2 + CH_3O \rightleftharpoons CH_3 + H_2NO$ (r13)	6.80E14	0.11	2332	[36]
$CH_2OH (+M) \rightleftharpoons CH_2O + H (+M)$ (r14)	7.4E10	0.811	38559	[37]
$CH_3 + N \rightleftharpoons HCNH + H$ (r15)	1.20E11	0.52	3.672E2	[38]
$CH_3 + N \rightleftharpoons HCN + H_2$ (r16)	7.1E12	0.00	0	[38]
$CH_4 + NH_2 \rightleftharpoons CH_3 + NH_3$ (r17)	1.2E13	0.00	1.515E04	[38]
$CH_2 (S) + N_2 \rightleftharpoons CH_2 + N_2$ (r18)	1.5E13	0.00	6.0E02	[38]
$CN + CH_4 \rightleftharpoons HCN + CH_3$ (r19)	9.0E04	2.64	−3.0E0	[38]
$H_2NO + CH_3 \rightleftharpoons CH_3O + NH_2$ (r20)	2.0E13	0.00	0.0E0	[38]
$H_2NO + N_2H_2 \rightleftharpoons NNH + NH_2OH$ (r21)	4.80E06	2.0	−1,19E3	[23]
$HNO + H_2NO \rightleftharpoons NO + NH_2OH$ (r22)	2.40E06	2.0	−1.19E3	[23]
$CH + CO_2 \rightleftharpoons HCO + CO$ (r23)	0.03	4.44	−3537	[39]
$NH_2OH (+M) \rightleftharpoons NH_2 + OH (+M)$ (r24)	1.4E20	−1.31	64080	[40]
$H_2NO + NH_2 \rightleftharpoons HNO + NH_3$ (r25)	3.0E12	0.00	1000	[40]
$CH_3 + NO \rightleftharpoons HCN + H_2O$ (r26)	2.4E12	0.00	1.57E04	[41]
$CH_3 + HNO \rightleftharpoons NO + CH_4$ (r27)	1.47E11	0.76	3.48E02	[41]
$CH_2 + NO \rightleftharpoons HCNO + H$ (r28)	3.8E13	−0.36	5.76E02	[41]
$CH_2 + NO \rightleftharpoons HCN + OH$ (r29)	1.0E14	0.00	0.0E0	[41]

without O_2. To study the impact of oxygen, for a NH_3/CH_3OH ratio of 1, sets 3–5, different initial O_2 concentrations were added. Experiments 4 and 4R are repeated experiments to evaluate repetitiveness. Finally, several experiments were carried out varying λ between 0.5 and 2, and the NH_3/CH_3OH ratio in the range of 0.6–10 to cover a wide range of conditions.

3. Kinetics

The mechanism from previous work on DME/NH_3 and DME/NH_3/NO mixtures has been used as the base mechanism [31]. This mechanism is primarily based on Glarborg et al. [32] as a basis. There are some minor updates for NH_3 [30], CH_3CN [33] and NH_3-NO [34] subsets, as detailed by Alzueta et al. [35]. Additionally, reactions of the DME subset, proposed by Marrodán et al. [5], have been incorporated.

With all the modifications described above, the model had major discrepancies in simulating the experimental conditions described in this work. The main discrepancy was the oxidation of CH_3OH, which occurred at higher temperatures than those observed experimentally. Therefore, the incorporation of reactions in which the NH_2 radical interacts with methanol was considered, following the work of Wang et al. [25] and Li et al. [28], together with new interactions between compounds generated from hydrogen abstraction in methanol by nitrogenous compounds [36] or their decomposition [37]. The inclusion of these reactions improved the ignition temperature of methanol oxidation, without noticeable modifications for ammonia.

Interactions between nitrogen and carbon compounds have also been added [38], which are responsible for improving the description of CH_4 and CO profiles. Table 2 shows the main updates for the CH_3OH subset.

Overall, the inclusion of the reactions in Table 2 has improved the prediction of the different species during the conversion of the NH_3/CH_3OH mixture. The kinetic model used includes a total of 484 species and 3155 reactions, and the simulations have been carried out using the Chemkin-Pro 2023 software [42] with the Pug Flow Reactor (PFR) module.

4. Results and discussion

In this work, mass balances were performed for all experiments, and representative examples are provided in Fig. S3 in the Supplementary Material. A thorough explanation of the interpretation of mass balances can also be found in the supplementary material. Carbon balances show low errors (<10%) overall, even though the non quantification of CH_2O is probably the reason for the higher errors found between 1025 and 1225 K. Nitrogen balances exhibit errors below 10%, and are lower in most of the temperature range considered. In conclusion, the good performance of mass balances is an indication that the main species involved in NH_3/CH_3OH conversion were considered, with the exception of CH_2O which was not quantified experimentally.

4.1. Pyrolysis of the NH_3/CH_3OH mixtures

Fig. 1 shows the experimental and calculated conversion of NH_3 and CH_3OH as a function of temperature in the absence of oxygen, for two different NH_3/CH_3OH ratios. From now on, experiments are denoted by symbols and calculations by lines. Both experimental data and model calculation coincide reasonably well, even though experimentally, the ammonia concentration decreased by around 5% within the temperature range of 1000–1175 K, while calculations predict an ammonia conversion of around 1%.

The main culprit in oxidising ammonia in these cases is the H radical, although it is in a smaller proportion than the capacity of CH_3OH to convert back NH_2 into NH_3. A reaction rate analysis was carried out at 1100 K under pyrolysis conditions, showing that the interaction between ammonia and the H radical is the most important in ammonia consumption. On the other hand, the interaction between NH_2 radical and CH_3OH recycles back a fraction of ammonia.

Methanol profiles are very well described by the model, Fig. 1B. The initial consumption of methanol, at approximately 1000 K, occurs through $CH_3OH (+M) \rightleftharpoons CH_3 + OH (+M)$ (r30), and $CH_3OH + H \rightleftharpoons CH_2OH + H_2$ (r31). Once the radical pool is built up, reaction (r31) becomes dominant. Most of the conversion of methanol proceeds in the 1000–1200 K temperature interval for the conditions of Fig. 1B. At the onset of the methanol reaction (1000 K), the reaction contributing the highest amount of H radicals is $CH_2OH \rightleftharpoons CH_2O + H$ (r32). However, as the temperature increases, $HCO (+M) \rightleftharpoons H + CO (+M)$ (r33) becomes the dominant reaction contributing the highest proportion of H radicals (1100–1200 K), which as mentioned above are very important in the conversion of NH_3.

In the presence of NH_3, the $NH_2 + CH_3OH \rightleftharpoons NH_3 + CH_2OH$ (r7) reaction contributed as well to methanol conversion once the temperature was high enough to allow the conversion of NH_3 into NH_2 radical. A sensitivity analysis for methanol at 1033 K can be found in Fig. S4 of the Supplementary Material, and indicates that the conversion of methanol is affected by reactions only involving NH_3 and thus the importance of the radical pool composition for the pyrolysis of the mixtures considered. However, the NH_3/CH_3OH ratio does not significantly affect the decomposition of NH_3 under pyrolysis conditions, and its increase slightly accelerates the thermal decomposition of CH_3OH at low temperatures. This can be observed in Fig. 1A, where the net ammonia profile is similar to the one observed for the NH_3/CH_3OH mixture. This is because the properties of the mixture become more similar to methanol with higher percentages of methanol in the mixture, leading to similar ignition properties of net methanol.

In addition, pure methanol decomposes at a lower temperature compared to the mixtures, because no interactions with nitrogen compounds inhibit methanol decomposition, both of which are found to be related to the consumption of radical H, i.e. $NH_2 + H (+M) = NH_3 (+M)$ (r34), and $NH_3 + H = NH_2 + H_2O$ (r35).

4.2. Oxidation of the NH_3/CH_3OH mixtures

4.2.1. Influence of the oxygen excess ratio

The influence of oxygen excess ratio (λ) on the conversion of NH_3 and CH_3OH has been studied and, as an example, results for a given NH_3/CH_3OH ratio of 1 are discussed. Fig. 2 shows the profiles of the most

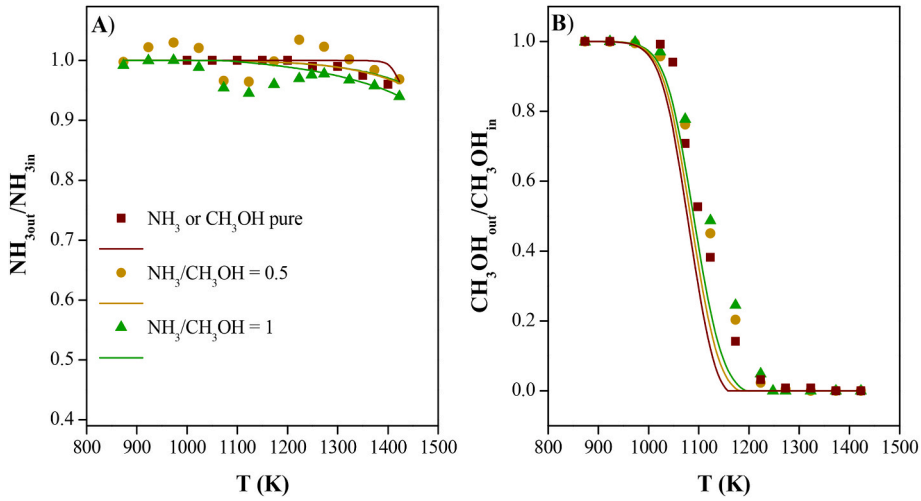

Fig. 1. Concentrations of A) NH_3, and B) CH_3OH as a function of temperature for different NH_3/CH_3OH ratios. Data for pyrolysis of pure ammonia conversion are taken from Abián et al. [30]. Sets 1, 2, 12 and 13 are taken from Table 2.

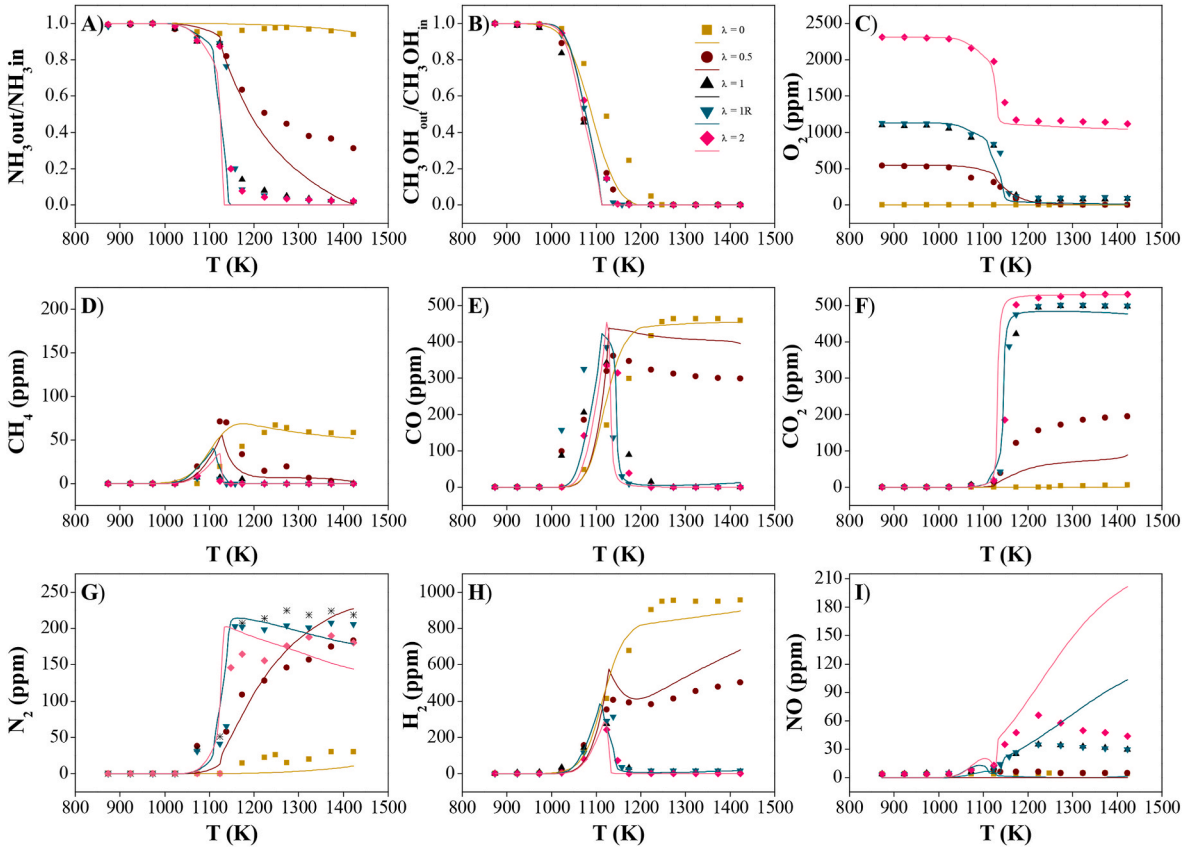

Fig. 2. Concentrations of the most important product species for $NH_3/CH_3OH = 1$ for different λ (Sets 1, 3–5 of Table 2).

significant species observed in the experiments quantified in this study. An example with all the compounds analysed (set 5) can be found in Fig. S5 of the Supplementary Material.

It is noted that ammonia concentration is significantly influenced by the O_2 excess ratio used, with complete oxidation of ammonia being observed between 1275 and 1300 K for stoichiometric and fuel-lean conditions. The oxidation range of NH_3 occurs between the temperatures 1025–1325 K. This is not the case for pyrolytic conditions, as mentioned in the previous section, nor fuel-rich conditions. In fuel-rich conditions, 60–70% conversion is reached between 1325 and 1425 K.

The model predicts well the conditions where the O_2 in the medium is sufficient to oxidise both fuels, but not for fuel-rich conditions, where above 1225 K it overestimates the NH_3 oxidation produced. To explain the overestimation of NH_3 consumption in fuel-rich conditions, the calculations performed at 1325 K will be presented. The most important reactions in the inhibition of ammonia oxidation are $CH_3 + H (+M) \rightleftharpoons CH_4 (+M)$ (r36), $CH_3OH + H \rightleftharpoons CH_3 + H_2O$ (r37), $H + H_2O \rightleftharpoons OH + H_2$ (-r38) and $NH_2 + H (+M) \rightleftharpoons NH_3 (+M)$ (r34). The consumption of H radicals through a pathway different from methanol abstraction (r7, r33, and r36) will be detrimental because this reaction is the most influential

in NH_3 oxidation. Reaction (r37) is inhibitory because it reduces the NH_2 radical back to NH_3 and competes with methanol for H consumption. This occurs because reactions involving the H radical, such as $CH_3OH + H \rightleftharpoons CH_2OH + H_2$ (r31) and $NH_2 + H \rightleftharpoons NH + H_2$ (r39), are highly relevant for the oxidation of ammonia. Therefore, it seems that the concentration and fate of the H radical, which participates in several key reactions, is very relevant also for the oxidation of ammonia, as was found for its pyrolysis. H concentration largely detriments the consumption of NH_3 under the studied conditions. So, small variations and small imprecisions in its prediction may affect strongly the calculations.

In Fig. 3, a sensitivity analysis for the NH_3 species can be seen for three values of λ, at the temperatures when 10% of NH_3 is consumed. As usually occurs during the oxidation of ammonia, reaction $H + O_2 \rightleftharpoons OH + O$ (r4) is one of the reactions that most favours its oxidation, due to the huge impact of O and OH radicals input to the radical pool. This is in agreement with Zhuang et al. [22], where it is also indicated that (r4) is the reaction that mostly promotes the oxidation of NH_3. Methanol also plays a key role in the oxidation of NH_3, with seven of the most favourable reactions including methanol derived compounds. In the oxidation of methanol, both OH and HO_2 radicals, in reactions $CH_3OH + OH \rightleftharpoons CH_2OH + H_2O$ (r7) and $CH_3OH + HO_2 \rightleftharpoons CH_2OH + H_2O_2$ (r1), and those originated by the NH_2 radical conversion, $NH_2 + CH_3OH \rightleftharpoons NH_3 + CH_3O$ (r6) and $NH_2 + CH_3OH \rightleftharpoons NH_3 + CH_2OH$ (r7) are the reactions that favour the oxidation of methanol. The presence of CH_3OH has also been reported as an important factor in other studies [24,25], although the importance of the interactions of CH_3OH with HO_2 and OH varies depending on the specific conditions considered.

The fact that reactions (r6) and (r7) favour the oxidation of ammonia may seem contradictory. Still, it is the early initial consumption of CH_3OH which causes the oxidation of NH_3 to occur at a lower temperature. Therefore, reactions that favour the oxidation of CH_3OH will lead to a shift of the oxidation of NH_3 to lower temperatures. NH_3 concentration is most sensitive to the above mentioned reactions in fuel-lean environments, except to the reaction involving the NH_2 radical, to which NH_3 concentrations are only sensitive when both fuels are present in similar concentrations.

CH_2OH and HCO are also important in the oxidation of NH_3, since their decomposition reactions, $CH_2OH \rightleftharpoons CH_2O + H$ (r32) and $HCO (+M) \rightleftharpoons H + CO (+M)$ (r33) generate hydrogen radicals and do not remove O_2 from the medium, thus favouring the oxidation of NH_3. (r9) was also found relevant in the atmospheric pressure study of Zhuang et al. [22]. On the other hand, if these compounds consume O_2, i.e. through $CH_2OH + O_2 \rightleftharpoons CH_2O + HO_2$ (r40) and $HCO + O_2 \rightleftharpoons CO + HO_2$ (r41), their presence harms the oxidation of fuels. Those reactions are among the ones that inhibit most the consumption of NH_3. Another reaction that causes a delay in the conversion of ammonia is $NH_3 + OH \rightleftharpoons NH_2 + H_2O$ (r3). While apparently this seems to be a contradiction, this happens because, at the start of the reaction, NH_3 and CH_3OH compete for OH radicals, which causes a delay in the consumption of methanol, and thus an overall delay in the consumption of the fuel mixture. This is further corroborated by some studies such as the ones by Li et al. [28] and Wang et al. [25], which propose that (r3) inhibits the ignition of ammonia, resulting in higher IDT's and a comparatively lower oxidation of NH_3.

Methanol starts to oxidise at 1025 K, and the reaction window where its oxidation occurs is narrower than the one observed for NH_3 (1025–1275 K). Within this temperature range, CH_3OH is consumed, even under pyrolysis conditions. At the beginning of the reaction, the experiment under fuel-lean conditions shows a lower conversion compared to the experiments conducted with other λ values. CH_3OH is oxidised at the same temperatures for both stoichiometric and fuel-lean conditions. The model captures the oxidation of CH_3OH reasonably well, overestimating the methanol consumption above 1125 K.

To clarify the behaviour of CH_3OH, a sensitivity analysis at the start of the reaction (10% conversion of CH_3OH) is shown in Fig. 4. The reactions with HO_2 and OH: $CH_3OH + HO_2 \rightleftharpoons CH_2OH + H_2O_2$ (r1) and $CH_3OH + OH \rightleftharpoons CH_2OH + H_2O$ (r42), are the most important ones in the oxidation of CH_3OH. The reaction $H + O_2 \rightleftharpoons OH + O$ (r4) also plays a significant role in fuel oxidation, as it increases the radical concentration in the radical pool. Zhuang et al. [22] did not identify (r1) and (r17) as the reaction that mostly promotes CH_3OH oxidation. However, this discrepancy may be attributed to lower NH_3/CH_3OH working ratios, since as Yin et al. [24] specify, the presence of HO_2 becomes more influential with decreasing NH_3/CH_3OH ratios.

The NH_2 radical also plays an important role in methanol consumption, with CH_3OH abstraction being the most sensitive for the $NH_2 + CH_3OH \rightleftharpoons NH_3 + CH_2OH$ (r7) reaction. It is observed that in most reactions that favour methanol consumption, the hydrogen atom is extracted from a C-H bond, not from the alcohol functional group. This is reasonable due to the lower energy requirement to break this kind of bond.

Concerning the inhibition of CH_3OH, the consumption of OH radicals by ammonia is the most inhibitory reaction, due to the competition between the two fuels for this radical. The consumption of O_2 by CH_2OH is crucial in reducing the consumption of CH_3OH, as the decomposition

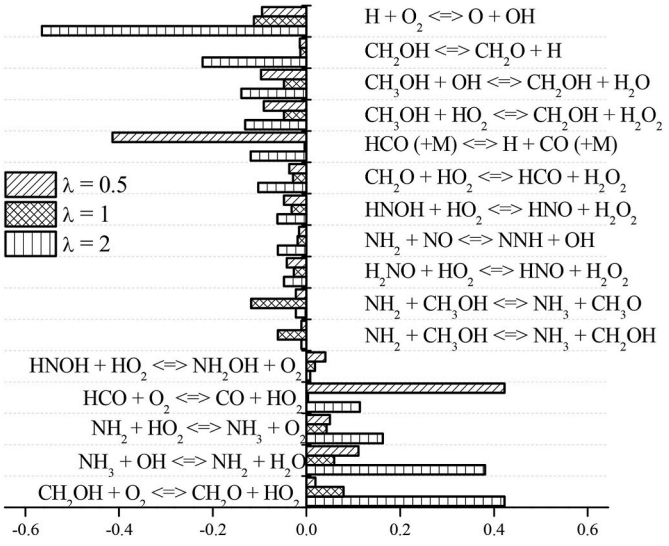

Fig. 3. Sensitivity analysis for NH_3 at 10% conversion of NH_3 for different λ. In ascending order of λ, the temperatures used for the analyses are 1125 K, 1108 K and 1083 K. Sets 3–5 in Table 2.

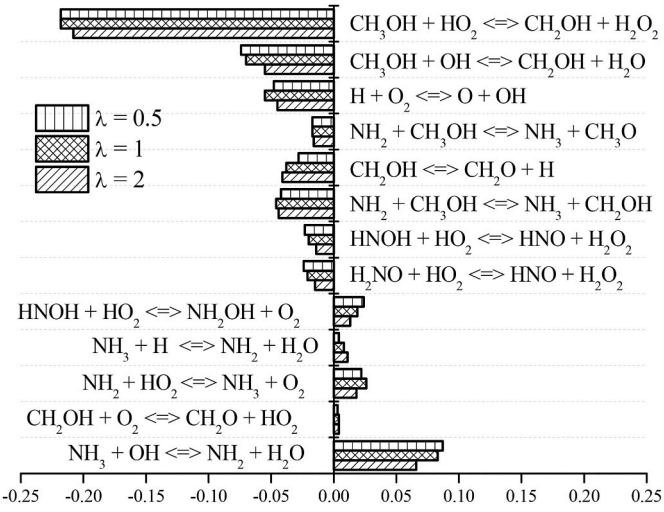

Fig. 4. Sensitivity analysis of CH_3OH at 10% CH_3OH consumed for different λ. In ascending order of λ, the temperatures used for the analyses are 1033 K, 1035 K and 1028 K. Sets 3–5 in Table 2.

of CH_2OH generating CH_2O and H effectively promotes the oxidation of both fuels.

The formation of a few nitrogen oxides during the conversion of NH_3/CH_3OH mixtures may be of concern. In the conditions of the present work, only NO, Fig. 2I, and small amounts of N_2O (not shown) have been attained.

For fuel-rich conditions, no relevant NO concentrations have been detected. This does not occur for cases with sufficient O_2 to oxidise both fuels ($\lambda \geq 1$). Increasing the initial O_2 concentration leads to an increase in NO emissions. In the higher emission conditions ($\lambda = 2$), the maximum NO concentration measured was 66 ppm (at 1225 K). This represents almost double the emission obtained under stoichiometric conditions (35 ppm NO at a temperature of 1225 K). This is consistent with other studies conducted at atmospheric pressure [22] or with similar setups [24], which report low N_2O and NO concentrations relative to the ammonia concentrations used.

Calculations indicate for $\lambda \geq 1$ that the reaction leading to the highest NO production is $HNO + H \rightleftharpoons NO + H_2$ (r43), with HNO originated from the reactions $H_2NO + H \rightleftharpoons HNO + H_2$ (r44), $H_2NO + NH_2 \rightleftharpoons HNO + NH_3$ (r45), $NH_2 + O \rightleftharpoons HNO + H$ (r46), and $NO + H (+M) \rightleftharpoons HNO (+M)$ (r47). Other production reactions are $CH_3 + NO \rightleftharpoons H_2CN + OH$ (-r48), $CH_3 + HNO \rightleftharpoons NO + CH_4$ (r49) and $HNO + O \rightleftharpoons NO + OH$ (r50).

Another set of significant reactions for NO are those involving NO-NO_2 interconversion, which occurs through $NO + O (+M) \rightleftharpoons NO_2 (+M)$ (r51) and $NO + HO_2 \rightleftharpoons NO_2 + OH$ (r52), and the formation of NO by $NO_2 + H \rightleftharpoons NO + OH$ (r53). The NO-NO_2 interconversion intensifies at elevated temperatures, decreasing the impact of NO reduction reactions in the background.

N_2 is the main nitrogen product of ammonia oxidation. Fig. 2G shows that the highest N_2 production occurs for $\lambda = 1$. This is because, with excess O_2, some NO is additionally produced, which decreases the nitrogen available for N_2 formation. Under fuel-rich conditions, both in experimental results and calculations, there is a progressive increase in N_2 concentration. However, for $\lambda \geq 1$ a sharp increase in N_2 concentration at 1175 K is observed. Above this temperature, the N_2 concentration remains practically constant for $\lambda = 1$. For $\lambda = 2$, N_2 concentration increases, albeit slightly.

The oxidation of CH_3OH generates some carbon compounds over the entire working temperature range. The most relevant compounds are CH_4, CO and CO_2. Although HCN has been analysed in the experiments, the quantified concentrations never exceeded 10 ppm, so it can be considered negligible. This has been confirmed in the study by Zhuang et al. [22], where the presence of HCN is minimal. This is because the CH_3OH intermediates do not show significant reactions that could lead to the synthesis of HCN, i.e. CH_2NH. This can be shown in Fig. 5.

Regarding CH_4, there is a wide range of temperatures at which it can be observed. Within the experiments of pyrolysis conditions, CH_4 starts to be quantified from 1075 K, with a range of occurrence which depends on the working λ. Under fuel-rich conditions, CH_4 is detected up to 1375 K, which does not occur for $\lambda \geq 1$, as it is completely consumed above 1150 K.

With respect to CO and CO_2, it is observed that calculations reproduce generally well the experimental behaviour, except for $\lambda = 0.5$, where there is an overestimation of CO, and, an underestimation of CO_2 is observed in calculations at the highest temperatures. Similar behaviour was observed by Wang et al. [25] in a multi-modal study. However, it has to be mentioned that the sum of CO and CO_2 is properly predicted by the model.

Fig. 5 shows the reaction pathways determined for different stoichiometries and a fuel NH_3/CH_3OH ratio of 1. The temperature at which the reaction rate analysis is made corresponds to the value for approximately 10% conversion of each fuel.

The consumption of methanol occurs mainly by reaction with OH and H radicals. Oxidation occurs mainly by H-abstraction, with the abstraction of an H radical from the C-H bond as the most important pathway. Thus, the compound that forms most abundantly from the oxidation of CH_3OH is CH_2OH. CH_3O forms also, but most importantly under fuel-rich conditions in the presence of CH_3 radicals. Interactions with NH_3 are not important at this point of the reaction. For a given temperature, as seen in Fig. 2B, the conversion of CH_3OH is completed at lower temperatures compared to the oxidation of NH_3. This is the reason for the low impact of NH_3 on CH_3OH oxidation.

The interaction of CH_3OH with NH_2 radicals, although it appears under all conditions studied as reactions that consume CH_3OH, the $NH_2 + CH_3OH \rightleftharpoons NH_3 + CH_3O$ (r6) reaction does not exceed roughly 3 % of CH_3OH consumption. In comparison, $NH_2 + CH_3OH \rightleftharpoons NH_3 + CH_2OH$ (r7) represents consumption of more than 7 % for either of the two cases.

CH_2OH decomposes by reactions $CH_2OH \rightleftharpoons CH_2O + H$ (r32) and $CH_2OH + O_2 \rightleftharpoons CH_2O + HO_2$ (r40) to form formaldehyde (CH_2O), although under fuel-rich conditions, CH_3O will also form CH_2O through thermal decomposition. CH_2O forms HCO by reaction with H and OH radicals, i.e. $CH_2O + H \rightleftharpoons HCO + H_2$ (r54) and $CH_2O + OH \rightleftharpoons HCO +$

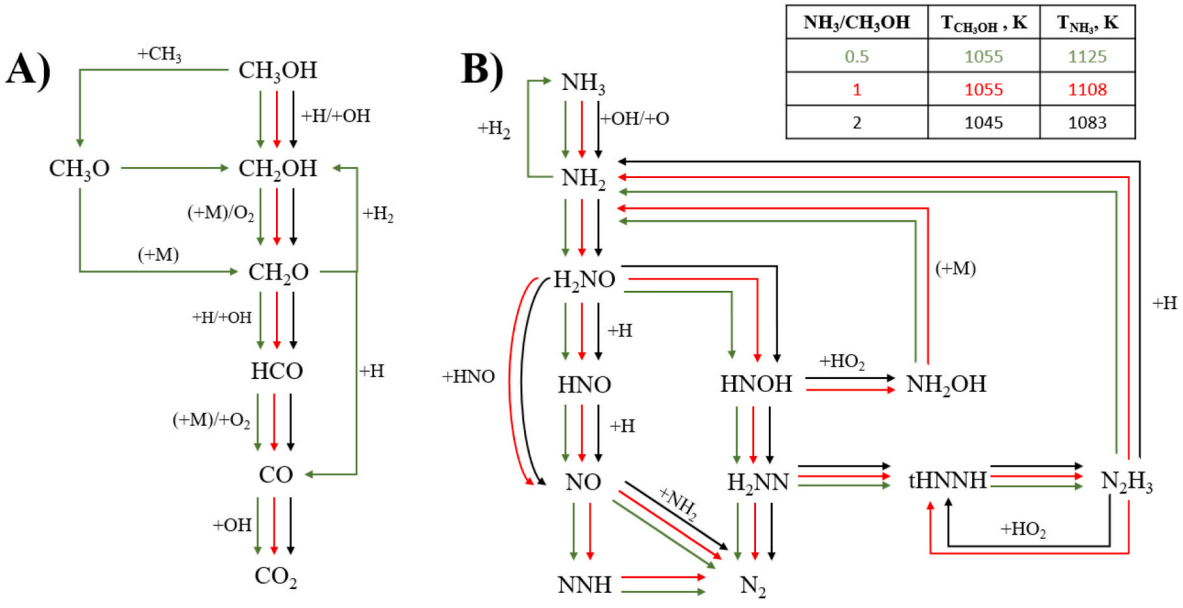

NH_3/CH_3OH	T_{CH_3OH}, K	T_{NH_3}, K
0.5	1055	1125
1	1055	1108
2	1045	1083

Fig. 5. Reaction pathways of A) CH_3OH and B) NH_3 conversion at different λ.

H_2O (r55), and it can also form CO by reaction with H radicals, $CH_2O + H \rightleftharpoons H + CO + H_2$ (r56). Again, the above leads to the conclusion that H radicals play an important role in the conversion of CH_2O, as a relevant intermediate in the oxidation of CH_3OH. Finally, carbon monoxide is oxidised to CO_2 through its reaction with OH radicals.

As a result, the most important reaction path for all the conditions studied is: $CH_3OH \rightarrow CH_2OH/CH_3O \rightarrow CH_2O \rightarrow HCO \rightarrow CO \rightarrow CO_2$ (reaction pathway 1). This reaction pathway is similar to those proposed by other authors [25,28,43]. Calculations further indicate that CH_3OH oxidates in a similar way for $\lambda \geq 1$. Although for fuel-rich conditions some variations are observed, as shown in Fig. 5: namely the interaction of CH_3OH with CH_3 radicals, $CH_3OH + CH_3 \rightleftharpoons CH_3O + CH_4$ (r57), followed by $CH_3O + H$ (+M) $\rightleftharpoons CH_3OH$ (+M) (r58), CH_3O (+M) $\rightleftharpoons CH_2O + H$ (+M) (r59), $CH_2O + H_2 \rightleftharpoons CH_2OH + H$ (r60), and $CH_2O + H \rightleftharpoons H + CO + H_2$ (r56).

In the case of NH_3, ammonia is oxidised due to OH and O radicals. This is not usually the case in the study of other mixtures such as DME-NH_3, where the oxidation reactions of NH_3 with O radicals are not relevant [31]. The oxidation of NH_3 produces NH_2. NH_2 radicals form H_2NO in the presence of NO or HO_2. The HO_2 radical comes from the reactions $CH_2OH + O_2 \rightleftharpoons CH_2O + HO_2$ (r40) and $HCO + O_2 \rightleftharpoons CO + HO_2$ (r41), showing that methanol generates radicals that favour this particular reaction pathway in the oxidation of ammonia. The H_2NO species has been mentioned to be a very important intermediate species during ammonia oxidation [30] and it appears to be also important during the combustion of NH_3/CH_3OH mixture, as seen in the present results. From H_2NO, a series of different branches is found to happen depending on λ:

For $\lambda \geq 1$,

$H_2NO \rightarrow NO \rightarrow N_2$ (reaction pathway 2)

Reaction pathway 2 generates NO directly through the reaction of H_2NO and HNO by $HNO + H_2NO \rightleftharpoons NO + NH_2OH$ (r22). Subsequently, this NO basically reacts with NH_2 radicals, forming N_2.

For $\lambda = 1$,

$H_2NO \rightarrow NO \rightarrow NNH \rightarrow N_2$ (reaction pathway 3)

Reaction pathway 3 is initially governed by (r22) but NO now interacts with NH_2 producing NNH radical through, $NH_2 + NO \rightleftharpoons NNH + OH$ (r62). NNH further decomposes into N_2 and H radicals.

For $\lambda \leq 1$,

$H_2NO \rightarrow HNO \rightarrow NO \rightarrow NNH \rightarrow N_2$ (reaction pathway 4)

For all λ,

$H_2NO \rightarrow HNO \rightarrow NO \rightarrow N_2$ (reaction pathway 5)

$H_2NO \rightarrow HNOH \rightarrow H_2NN \rightarrow N_2$ (reaction pathway 6)

$H_2NO \rightarrow HNOH \rightarrow H_2NN \rightarrow tHNNH \rightarrow N_2H_3 \rightarrow NH_2$ (reaction pathway 7)

Although reaction pathways 4 and 5 generate NO at some point in the reaction, they are pathways that favour the complete oxidation of NH_3, generating N_2. The same occurs in reaction pathway 6. In this case, N_2 is formed without NO as an intermediate. The reaction pathway 7 again produces NH_2 radicals. For this purpose, all compounds forming this pathway are thermally decomposed, except N_2H_3, which interacts

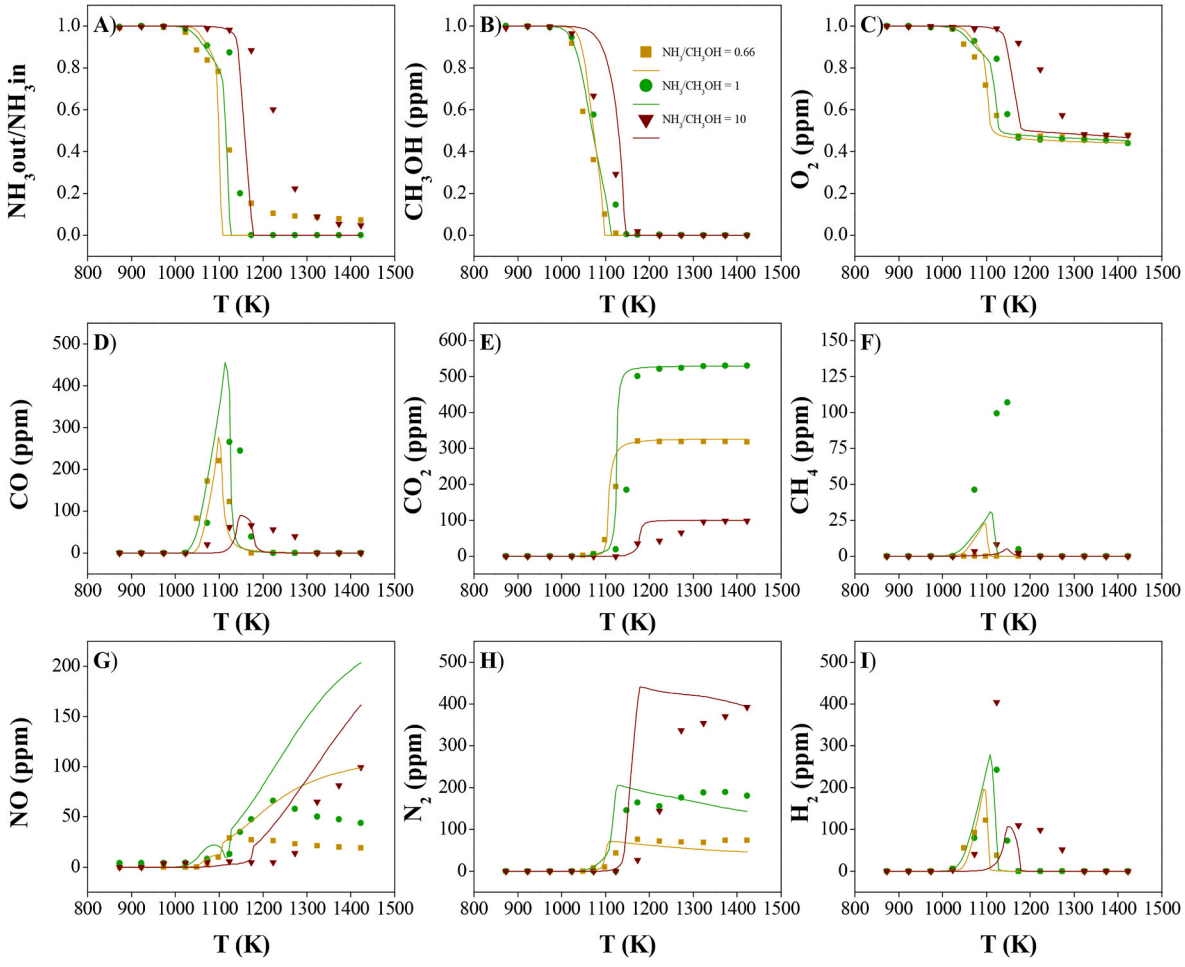

Fig. 6. Concentration profiles of the most important species at $\lambda = 2$ for different NH_3/CH_3OH ratios (Sets 5, 8 and 9 of Table 2).

with the H and HO_2 radicals, giving the reactions $N_2H_3 + H \rightleftharpoons 2NH_2$ (r63), and $N_2H_3 + HO_2 \rightleftharpoons H_2O_2 + tHNNH$ (r64). The reaction (r64) still favours the consumption of fuels, because, as mentioned above, a large amount of OH radicals are produced from H_2O_2.

4.2.2. Influence of the NH_3/CH_3OH ratio

The present section will focus on understanding the impact of using different NH_3/CH_3OH ratios on the conversion of the mixtures and the formation of products. Fig. 6 shows the concentration of the measured compounds as a function of the temperatures for the three different NH_3/CH_3OH ratios considered. Examples of others λ can be found in Figs. S6–S7 of the Supplementary Material.

Referring to the behaviour of the fuels, it is noted that both compounds oxidise at lower temperatures as the proportion of CH_3OH in the medium increases. NH_3 is highly affected by the presence of an elevated concentration of CH_3OH. Fig. 6A shows a 100 K difference between $NH_3/CH_3OH = 10$ and $NH_3/CH_3OH = 0.6$, achieving complete oxidation of ammonia at lower temperatures with the increase of CH_3OH in the mixture (150 K less). No noticeable difference has been observed when changing the stoichiometry for a given NH_3/CH_3OH ratio, where the differences between fuel-rich and fuel-lean conditions were only about 25 K. This behaviour is also captured properly by calculations. For the case of $NH_3/CH_3OH = 10$, the calculations overestimate the oxidising capacity of ammonia, resulting in a difference of 150 K for the complete oxidation of NH_3.

The most important NH_3 consumption reactions include interaction with OH and O radicals: $NH_3 + OH \rightleftharpoons NH_2 + H_2O$ (r3) and $NH_3 + O \rightleftharpoons NH_2 + OH$ (r65). A fraction of the NH_2 radicals is recycled back to NH_3. The most relevant NH_3 production reaction is $NH_2 + HO_2 \rightleftharpoons NH_3 + O_2$ (r66), so an increased production of HO_2 radical will lead to an inhibition of ammonia oxidation. This is in agreement with the sensitivity analyses carried out, where the most important reaction in the inhibition of both fuels is $CH_2OH + O_2 \rightleftharpoons CH_2O + HO_2$ (r40), which is also the most important HO_2 production reaction. For $NH_3/CH_3OH = 10$, comparatively, a lower amount of HO_2 is produced, which leads to a lower inhibition of NH_3 oxidation, which may be one of the factors affecting the overestimation of NH_3 consumption. This same fact was shown by Yin et al. [24]. Consequently, the decrease in importance of HO_2 formation causes other reactions to be more influential in the production of NH_3, as is the case for $tHNNH + NH_2 \rightleftharpoons NNH + NH_3$ (r67).

Fig. 6B shows the concentration of CH_3OH as a function of temperature. A clear influence is observed when modifying methanol concentrations. At 1175 K, complete oxidation of CH_3OH is achieved for $NH_3/CH_3OH = 0.6$. The same was not observed in the other cases, with 15% and 29% of CH_3OH reproducing for the NH_3/CH_3OH ratios of 1 and 10, respectively. The calculations reproduce well the experimental behaviour for $NH_3/CH_3OH \leq 1$, showing that ratios with a lower methanol concentration result in an underestimate of the methanol consumption. The difference between calculated and experimental values may be due to the lower OH concentration in the medium, and the sensitivity of results to the concentration of those radicals, since for $NH_3/CH_3OH \geq 1$, a higher concentration of OH radicals is produced and predictions are comparatively better. This is due to reactions such as $H_2O_2 (+M) \rightleftharpoons 2OH (+M)$ (r2) or $NO + HO_2 \rightleftharpoons NO_2 + OH$ (r52). In the work of Yin et al. [24], this pattern was also observed concerning (r2). Another evidence is the minor importance of $CH_3OH + OH \rightleftharpoons CH_2OH + H_2O$ (r42) for $NH_3/CH_3OH = 10$, with the reaction $CH_3OH + H \rightleftharpoons CH_2OH + H_2$ (r31) being the most important.

O_2 exhibits the same behaviour as presented for the fuels, with a reliable model representation of O_2 for NH_3/CH_3OH ratio of 1 and 0.66, Fig. 6C. However, the model overestimates O_2 consumption for small amounts of CH_3OH in the mixture, being consumed at lower temperatures in the calculations. The relevance of O_2-producing reactions, i.e. $NH_2 + HO_2 \rightleftharpoons NH_3 + O_2$ (r66) and $HNOH + HO_2 \rightleftharpoons NH_2OH + O_2$ (r68), decreases in importance when decreasing CH_3OH in the mixture. This may explain why the calculations overestimate the O_2 consumption when little methanol is present in the reacting mixture.

For CO and CO_2 (Fig. 6D and E), the model correctly represents the behaviour of both species. It only fails in the estimation of CO at low CH_3OH concentrations, because the temperature range in which this intermediate has been measured (1075–1275 K) is wider than the calculated one (1125–1233 K).

Fig. 6G shows the concentration of NO. The maximum NO concentration represented 15% of the nitrogen for the cases where $NH_3/CH_3OH \leq 1$. NO is mainly formed from HNO, as has been mentioned earlier, with some common reactions occurring always: $HNO + H_2NO \rightleftharpoons NO + NH_2OH$ (r22), $HNO + O_2 \rightleftharpoons HO_2 + NO$ (r69) and $HNO (+M) \rightleftharpoons NO + H (+M)$ (r70). However, the $HNO + H \rightleftharpoons NO + H_2$ (r43) reaction, which is the most important for the $NH_3/CH_3OH = 0.6$ case, is not even an important production reaction when the mixture contains the same concentration of both fuels. For $NH_3/CH_3OH = 10$, it is found that $HNO + H_2NO \rightleftharpoons NO + NH_2OH$ (r22) is not relevant in the NO production, with the rest of the above reactions being the most relevant ones.

The reactions that consume NO most rapidly include, for the three NH_3/CH_3OH ratios studied, $NH_2 + NO \rightleftharpoons NNH + OH$ (r62) and $NH_2 + NO \rightleftharpoons N_2 + H_2O$ (r71). $HCO + NO \rightleftharpoons HNO + CO$ (r72) is also relevant for the case of higher CH_3OH concentration, and $NH + NO \rightleftharpoons N_2 + OH$ (r73) when the NH_3 concentration is higher than the CH_3OH concentration. In all the cases, a maximum NO concentration is found, and is subsequently reduced with increasing temperature. A different behaviour occurs with the higher NH_3 concentration in the mixture studied, where NO starts to form at 1275 K, reaching its maximum concentration at 1425 K. This behaviour is similar to that observed when burning net NH_3 [30], with NO formation representing 10% of the added ammonia at the highest working temperatures.

Referring to H_2 (Fig. 6I), it is observed that the maximum concentration peaks are shifted on the temperature axis as a function of the NH_3/CH_3OH ratio. As concluded for previous cases, the behaviour of fuel mixtures with higher or equal concentrations of CH_3OH versus NH_3 does not change significantly, varying their maximum concentration in a temperature difference of 50 K. This does not occur for $NH_3/CH_3OH = 10$, where the maximum H_2 concentration is shifted to 1175 K. Another difference to the other species measured is the temperature range in which H_2 has been observed, which is slightly wider (1025–1325 K) compared to what appear in calculations (1100–1175 K).

Fig. 7 shows the reaction pathways determined for both fuels when either the NH_3 and CH_3OH consumption represents 10% of the total added at the fuel lean condition ($\lambda = 2$). For methanol (Fig. 7A), the main reaction pathway is the same as previously proposed, $CH_3OH \rightarrow CH_2OH \rightarrow CH_2O \rightarrow HCO \rightarrow CO \rightarrow CO_2$ (reaction pathway 1). However, the modification of the NH_3/CH_3OH ratio implies the appearance of additional secondary pathways.

Increasing CH_3OH concentration ($NH_3/CH_3OH = 0.6$), a reaction pathway formatting of CH_2OH appears to be significant: $CH_3OH \rightarrow CH_3 \rightarrow CH_3ONO \rightarrow CH_3O \rightarrow CH_2OH$ (reaction pathway 8). This reaction pathway does imply interaction with nitrogen compounds, through the reactions: $CH_3 + NO_2 \rightleftharpoons CH_3ONO$ (r74), followed by $CH_3ONO (+M) \rightleftharpoons CH_3O + NO (+M)$ (r75).When the proportion of ammonia is much higher than that of methanol, $NH_3/CH_3OH = 10$, the above reaction pathway is not significant, although, together with the CH_3 radical, the production of CH_2OH and CH_2O by CH_3O is more relevant. The higher proportion of NH_3 in the mixtures also generates new interactions not present in other cases, such as: $CO + NH_2 \rightleftharpoons HNCO + H$ (r76) and $HNCO + NH_2 \rightleftharpoons NCO + NH_3$ (r77).

Regarding NH_3 (Fig. 7B), the main reaction pathways are similar to those presented above: $NH_3 \rightarrow NH_2 \rightarrow H_2NO \rightarrow HNO \rightarrow NO \rightarrow N_2$ (reaction pathway 11). For $NH_3/CH_3OH = 10$, NH_2 radicals react with tHNNH, through the reaction $tHNNH + NH_2 \rightleftharpoons NNH + NH_3$ (r67), resulting in an inhibition of ammonia consumption. In turn, N_2H_3 does not form NH_2 in these cases, but the NH_2 radical reacts instead with N_2H_4, through $NH_2 + N_2H_4 \rightleftharpoons N_2H_3 + NH_3$ (r78), which leads to an inhibition of ammonia oxidation. This leads to the conclusion that a lower proportion of CH_3OH

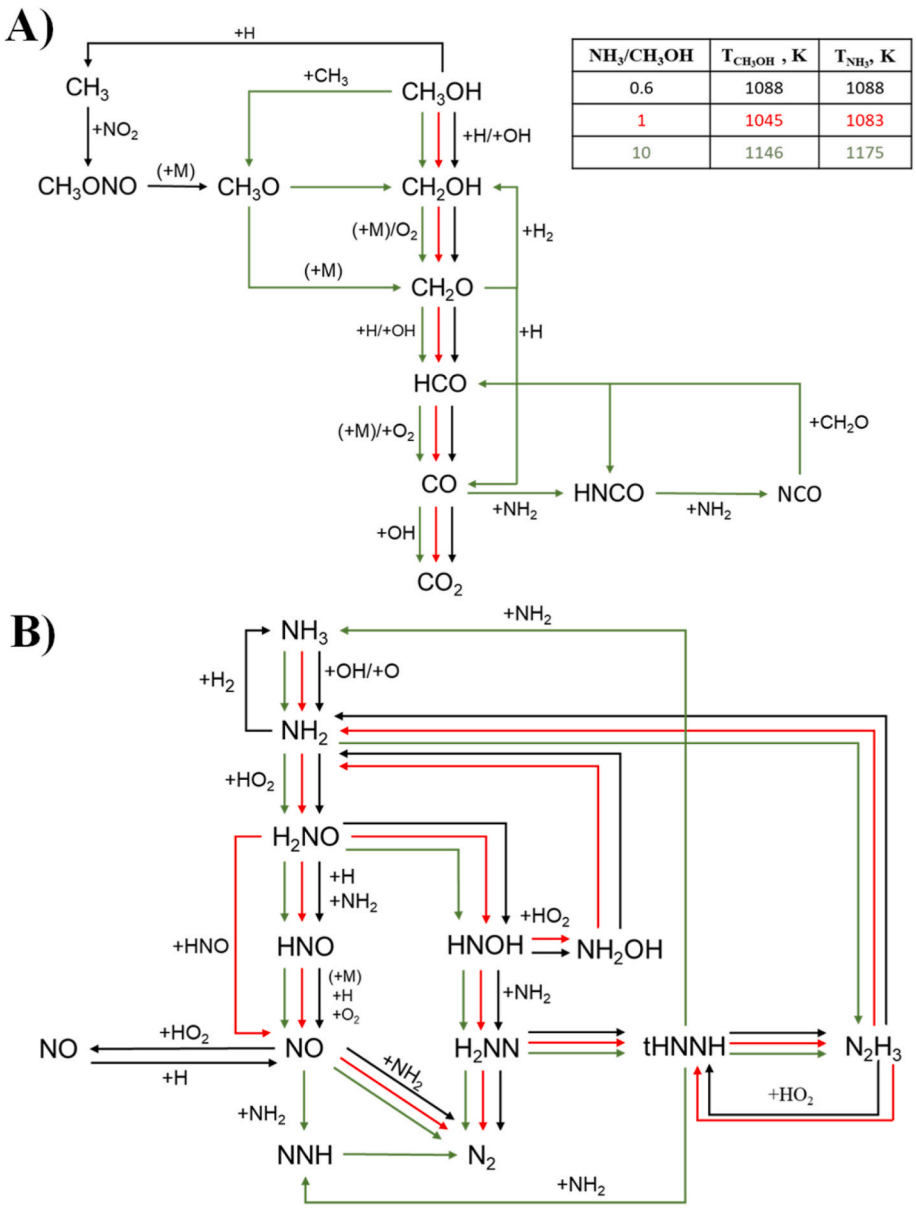

NH_3/CH_3OH	T_{CH_3OH}, K	T_{NH_3}, K
0.6	1088	1088
1	1045	1083
10	1146	1175

Fig. 7. Reaction pathways of A) CH_3OH and B) NH_3 for different NH_3/CH_3OH ratios.

in the medium makes reactions such as (r67) and (r68) more relevant, inhibiting thus the oxidation of NH_3.

In mixtures with higher CH_3OH concentration ($NH_3/CH_3OH = 0.6$), the NO-NO_2 interconversion is more important. The reactions showing that interconversion in this case are $NO + HO_2 \rightleftharpoons NO_2 + OH$ (r52), and $NO_2 + H \rightleftharpoons NO + OH$ (r53).

5. Conclusion

A comprehensive study of the conversion of NH_3/CH_3OH mixtures has been carried out. A quartz flow reactor, operating at atmospheric pressure, was used to perform experiments within a temperature range of 875–1425 K. The parameters varied during the study were λ (0–2) and the NH_3/CH_3OH ratio (0.6–10).

Stoichiometry, λ, is very determinant in the conversion of the mixtures. Fuel-lean conditions provide the best results in the oxidation of NH_3, reducing the temperature at which it is oxidised compared to stoichiometric and fuel-rich conditions. The H radical plays a key role in converting both fuels. The impact of CH_3OH presence on the oxidation of NH_3 has been evidenced. Due to the initial inhibition of NH_3, caused by competition for OH radicals of both fuels, CH_3OH oxidation, which is produced at comparatively lower temperatures, results in lowering the oxidation temperature to NH_3. The sensitivity analysis indicates that numerous carbon-containing compounds positively influence ammonia oxidation through their interactions.

The higher the CH_3OH initial concentration of the NH_3/CH_3OH mixture, the better the ammonia oxidation performance. When changing the NH_3/CH_3OH ratios from 0.6 to 10, NH_3 consumption is shifted to a lower temperature (up to 100 K). Also, the main reaction pathways during NH_3 and CH_3OH conversion have been shown to depend strongly on the NH_3/CH_3OH ratio.

Finally, it should be noted that the model used for the simulations is able to reproduce properly the experimental results obtained for $NH_3/CH_3OH \leq 1$, with the largest discrepancy observed in fuel-rich conditions. Therefore, further model development is desirable, in particular to reproduce more accurately the cases where the added methanol is rather small ($NH_3/CH_3OH = 10$).

CRediT authorship contribution statement

A. Ruiz-Gutiérrez: Writing – review & editing, Writing – original draft, Software, Methodology, Formal analysis, Data curation, Conceptualization. **I. De Diego:** Software, Methodology, Data curation. **M.U. Alzueta:** Writing – review & editing, Writing – original draft, Validation, Software, Resources, Project administration, Investigation, Funding acquisition, Formal analysis, Conceptualization.

Declaration of competing interest

The authors declare that they have no known competing financial interests or personal relationships that could have appeared to influence the work reported in this paper.

Acknowledgments

The authors express their gratitude to grant PID2021-12432OB-I00 and TED2021-129557B-I00, funded by MCIN/AEI/10.13039/501100011033, "ERDF A way of making Europe", by the "European Union" and to Aragón Government (Ref. T22_23R) and PRE2022-104181 grant funded by Ministry of Science and Innovation.

Appendix A. Supplementary data

Supplementary data to this article can be found online at https://doi.org/10.1016/j.biombioe.2024.107572.

Data availability

Data will be made available on request.

References

[1] Q. Zhang, R. Zhang, Y. Qi, Z. Wang, Ignition characteristics of ammonia-methanol blended fuel in a rapid compression machine, Fuel 368 (2024) 131636, https://doi.org/10.1016/j.fuel.2024.131636.
[2] S. Zhu, Q. Xu, R. Tang, J. Gao, Z. Wang, J. Pan, D. Zhang, A comparative study of oxidation of pure ammonia and ammonia/dimethyl ether mixtures in a jet-stirred reactor using SVUV-PIMS, Combust. Flame 250 (2023) 112643, https://doi.org/10.1016/j.combustflame.2023.112643.
[3] N. Campion, H. Nami, P.R. Swisher, P. Vang Hendriksen, M. Münster, Techno-economic assessment of green ammonia production with different wind and solar potentials, Renewable Sustainable Energy Rev. 173 (2023) 113057, https://doi.org/10.1016/j.rser.2022.113057.
[4] A. Hayakawa, T. Goto, R. Mimoto, T. Kudo, H. Kobayashi, NO formation/reduction mechanisms of ammonia/air premixed flames at various equivalence ratios and pressures, Mech. Eng. J. (2015) 14–402, https://doi.org/10.1299/mej.14-00402.
[5] L. Marrodán, Á. Millera, R. Bilbao, M.U. Alzueta, An experimental and modeling study of acetylene-dimethyl ether mixtures oxidation at high-pressure, Fuel 327 (2022) 125143, https://doi.org/10.1016/j.fuel.2022.125143.
[6] L. Marrodán, Á. Millera, R. Bilbao, M.U. Alzueta, Experimental and modeling evaluation of dimethoxymethane as an additive for high-pressure acetylene oxidation, J. Phys. Chem. A 126 (2022) 6253–6263, https://doi.org/10.1021/acs.jpca.2c03130.
[7] X. Shi, W. Li, J. Zhang, Q. Fang, Y. Zhang, Z. Xi, Y. Li, Exploration of NH_3 and NH_3/DME laminar flame propagation in O_2/CO_2 atmosphere: insights into NH_3/CO_2 interactions, Combust. Flame 260 (2024) 113245, https://doi.org/10.1016/j.combustflame.2023.113245.
[8] H. Xiao, H. Li, Experimental and kinetic modeling study of the laminar burning velocity of NH_3/DME/air premixed flames, Combust. Flame 245 (2022) 112372, https://doi.org/10.1016/j.combustflame.2022.112372.
[9] H. Li, H. Xiao, Experimental study on the explosion characteristics of NH_3/DME/air mixtures, Fuel 352 (2023) 129069, https://doi.org/10.1016/j.fuel.2023.129069.
[10] G. Issayev, B.R. Giri, A.M. Elbaz, K.P. Shrestha, F. Mauss, W.L. Roberts, A. Farooq, Ignition delay time and laminar flame speed measurements of ammonia blended with dimethyl ether: a promising low carbon fuel blend, Renew. Energy 181 (2022) 1353–1370, https://doi.org/10.1016/j.renene.2021.09.117.
[11] X. Meng, M. Zhang, C. Zhao, H. Tian, J. Tian, W. Long, M. Bi, Study of combustion and NO chemical reaction mechanism in ammonia blended with DME, Fuel 319 (2022) 123832, https://doi.org/10.1016/j.fuel.2022.123832.
[12] J. Chen, X. Gou, Experimental and kinetic study on the extinction characteristics of ammonia-dimethyl ether diffusion flame, Fuel 334 (2023) 126743, https://doi.org/10.1016/j.fuel.2022.126743.
[13] L. Dai, H. Hashemi, P. Glarborg, S. Gersen, P. Marshall, A. Mokhov, H. Levinsky, Ignition delay times of NH_3/DME blends at high pressure and low DME fraction: RCM experiments and simulations, Combust. Flame 227 (2021) 120–134, https://doi.org/10.1016/j.combustflame.2020.12.048.
[14] G. Yin, B. Xiao, H. Zhao, H. Zhan, E. Hu, Z. Huang, Jet-stirred reactor measurements and chemical kinetic study of ammonia with dimethyl ether, Fuel 341 (2023) 127542, https://doi.org/10.1016/j.fuel.2023.127542.
[15] G. Issayev, B.R. Giri, A.M. Elbaz, K.P. Shrestha, F. Mauss, W.L. Roberts, A. Farooq, Combustion behavior of ammonia blended with diethyl ether, Proc. Combust. Inst. 38 (2021) 499–506, https://doi.org/10.1016/j.proci.2020.06.337.
[16] A.M. Elbaz, B.R. Giri, G. Issayev, K.P. Shrestha, F. Mauss, A. Farooq, W.L. Roberts, Experimental and kinetic modeling study of laminar flame speed of dimethoxymethane and ammonia blends, Energy Fuels 34 (2020) 14726–14740, https://doi.org/10.1021/acs.energyfuels.0c02269.
[17] W. Guan, A. Abdelsamie, C. Chi, Z. He, D. Thévenin, A dedicated reduced kinetic model for ammonia/dimethyl-ether turbulent premixed flames, Combust. Flame 257 (2023), https://doi.org/10.1016/j.combustflame.2023.113002.
[18] K.P. Shrestha, B.R. Giri, A.M. Elbaz, G. Issayev, W.L. Roberts, L. Seidel, F. Mauss, A. Farooq, A detailed chemical insights into the kinetics of diethyl ether enhancing ammonia combustion and the importance of NO_x recycling mechanism, Fuel Communications 10 (2022) 100051, https://doi.org/10.1016/j.jfueco.2022.100051.
[19] Z. Wang, X. Han, Y. He, R. Zhu, Y. Zhu, Z. Zhou, K. Cen, Experimental and kinetic study on the laminar burning velocities of NH_3 mixing with CH_3OH and C_2H_5OH in premixed flames, Combust. Flame 229 (2021) 38, https://doi.org/10.1016/j.combustflame.2021.02.038.
[20] D. Zheng, D. He, Y. Du, M. Zhang, J. Li, Y. Ding, Z. Peng, Mid-infrared absorption spectroscopy measurements and model improvements during the oxidation of ammonia/ethanol and ammonia/diethyl ether blends in a shock tube, Fuel 357 (2024) 129635, https://doi.org/10.1016/j.fuel.2023.129635.
[21] S. Brynolf, M. Taljegard, M. Grahn, J. Hansson, Electrofuels for the transport sector: a review of production costs, Renewable Sustainable Energy Rev. 81 (2018) 1887–1905, https://doi.org/10.1016/j.rser.2017.05.288.
[22] Y. Zhuang, R. Wu, X. Wang, R. Zhai, C. Gao, An experimental and modeling study on the oxidation of ammonia-methanol mixtures in a jet stirred reactor, Fuel 356 (2024) 129628, https://doi.org/10.1016/j.fuel.2023.129628.
[23] M. Lu, D. Dong, F. Wei, W. Long, Y. Wang, L. Cong, P. Dong, H. Tian, P. Wang, Chemical mechanism of ammonia-methanol combustion and chemical reaction kinetics analysis for different methanol blends, Fuel 341 (2023) 127697, https://doi.org/10.1016/j.fuel.2023.127697.
[24] G. Yin, S. Shen, H. Zhan, E. Hu, H. Zhang, Y. Bao, Z. Huang, Experimental and modeling study for the effect of methanol blending on ammonia oxidation and NO_x formation at high pressure, Combust. Flame 268 (2024) 113654, https://doi.org/10.1016/j.combustflame.2024.113654.
[25] Z. Wang, B. Mei, N. Liu, A. Thawko, X. Mao, H. Zhao, P. Glarborg, S. J. Klippenstein, Y. Ju, High pressure ammonia/methanol oxidation up to 100 atm, Proc. Combust. Inst. 40 (2024) 105489, https://doi.org/10.1016/j.proci.2024.105489.
[26] K. Zhang, X. Ma, Z. Yu, Y. Li, S. Shuai, Microscopic insights into the ammonia-methanol blended combustion at high temperatures, Fuel 374 (2024) 132483, https://doi.org/10.1016/j.fuel.2024.132483.
[27] B. Wang, H. Wang, C. Yang, D. Hu, B. Duan, Y. Wang, Effect of different ammonia/methanol ratios on engine combustion and emission performance, Appl. Therm. Eng. 236 (2024) 121519, https://doi.org/10.1016/j.applthermaleng.2023.121519.
[28] M. Li, X. He, H. Hashemi, P. Glarborg, V.M. Lowe, P. Marshall, R. Fernandes, B. Shu, An experimental and modeling study on auto-ignition kinetics of ammonia/methanol mixtures at intermediate temperature and high pressure, Combust. Flame 242 (2022) 112160, https://doi.org/10.1016/j.combustflame.2022.112160.
[29] M.U. Alzueta, R. Pernía, M. Abián, Á. Millera, R. Bilbao, CH_3SH conversion in a tubular flow reactor. Experiments and kinetic modelling, Combust. Flame 203 (2019) 23–30, https://doi.org/10.1016/j.combustflame.2019.01.017.
[30] M. Abián, M. Benés, A. de Goñi, B. Muñoz, M.U. Alzueta, Study of the oxidation of ammonia in a flow reactor. Experiments and kinetic modeling simulation, Fuel 300 (2021) 120979, https://doi.org/10.1016/j.fuel.2021.120979.
[31] A. Ruiz-Gutiérrez, P. Rebollo, M.U. Alzueta, Combustion of NH_3/DME and NH_3/DME/NO mixtures, Fuel 381 (2024) 133253, https://doi.org/10.1016/j.fuel.2024.133253.
[32] P. Glarborg, J.A. Miller, B. Ruscic, S.J. Klippenstein, Modeling nitrogen chemistry in combustion, Prog. Energy Combust. Sci. 67 (2018) 31–68, https://doi.org/10.1016/j.pecs.2018.01.002.
[33] M.U. Alzueta, M. Guerrero, Á. Millera, P. Marshall, P. Glarborg, Experimental and kinetic modeling study of oxidation of acetonitrile, Proc. Combust. Inst. 38 (2021) 575–583, https://doi.org/10.1016/j.proci.2020.07.043.
[34] M.U. Alzueta, L. Ara, V.D. Mercader, M. Delogu, R. Bilbao, Interaction of NH_3 and NO under combustion conditions. Experimental flow reactor study and kinetic modeling simulation, Combust. Flame 235 (2022) 111691, https://doi.org/10.1016/j.combustflame.2021.111691.
[35] M.U. Alzueta, M. Abián, I. Elvira, V.D. Mercader, L. Sieso, Unraveling the NO reduction mechanisms occurring during the combustion of NH_3/CH_4 mixtures, Combust. Flame (2022), https://doi.org/10.1016/j.combustflame.2022.112531.
[36] A.M. Dean, J.W. Bozzelli, Combustion chemistry of nitrogen, in: W.C. Gardiner (Ed.), Gas-Phase Combustion Chemistry, Springer, NY, 2020, pp. 125–341. New, New York.
[37] A. Stagni, C. Cavallotti, S. Arunthanayothin, Y. Song, O. Herbinet, F. Battin-Leclerc, T. Faravelli, An experimental, theoretical and kinetic-modeling study of the gas-phase oxidation of ammonia, React. Chem. Eng. 5 (2020) 696–711, https://doi.org/10.1039/c9re00429g.

[38] X. Meng, L. Liu, M. Qin, W. Zhu, W. Long, M. Bi, Modeling and chemical kinetic analysis of methanol and reformed gas (H_2/CO_2) blending with ammonia under lean-burn condition, Int. J. Hydrogen Energy 58 (2024) 190–199, https://doi.org/10.1016/j.ijhydene.2024.01.150.
[39] Y. Song, H. Hashemi, J.M. Christensen, C. Zou, P. Marshall, P. Glarborg, Ammonia oxidation at high pressure and intermediate temperatures, Fuel 181 (2016) 358–365, https://doi.org/10.1016/j.fuel.2016.04.100.
[40] J. Otomo, M. Koshi, T. Mitsumori, H. Iwasaki, K. Yamada, Chemical kinetic modeling of ammonia oxidation with improved reaction mechanism for ammonia/air and ammonia/hydrogen/air combustion, Int. J. Hydrogen Energy 43 (2018) 3004–3014, https://doi.org/10.1016/j.ijhydene.2017.12.066.
[41] A.A. Konnov, Implementation of the NCN pathway of prompt-NO formation in the detailed reaction mechanism, Combust. Flame 156 (2009) 2093–2105, https://doi.org/10.1016/j.combustflame.2009.03.016.
[42] ANSYS Chemkin-Pro 2023 R1, ReactionDesign: San Diego (2023).